TISSUE ENGINEERING: Part A
Volume 20, Numbers 19 and 20, 2014

DOI: 10.1089/ten.tea.2013.0397

Anisotropic Poly(Ethylene Glycol)/Polycaprolactone Hydrogel–Fiber Composites for Heart Valve Tissue Engineering

Hubert Tseng, PhD,[1,*] Daniel S. Puperi, BS,[1,*] Eric J. Kim, BS,[1] Salma Ayoub, BS,[1] Jay V. Shah,[1] Maude L. Cuchiara, PhD,[2] Jennifer L. West, PhD,[2] and K. Jane Grande-Allen, PhD[1]

The recapitulation of the material properties and structure of the native aortic valve leaflet, specifically its anisotropy and laminate structure, is a major design goal for scaffolds for heart valve tissue engineering. Poly(ethylene glycol) (PEG) hydrogels are attractive scaffolds for this purpose as they are biocompatible, can be modified for their mechanical and biofunctional properties, and can be laminated. This study investigated augmenting PEG hydrogels with polycaprolactone (PCL) as an analog to the fibrosa to improve strength and introduce anisotropic mechanical behavior. However, due to its hydrophobicity, PCL must be modified prior to embedding within PEG hydrogels. In this study, PCL was electrospun (ePCL) and modified in three different ways, by protein adsorption (pPCL), alkali digestion (hPCL), and acrylation (aPCL). Modified PCL of all types maintained the anisotropic elastic moduli and yield strain of unmodified anisotropic ePCL. Composites of PEG and PCL (PPCs) maintained anisotropic elastic moduli, but aPCL and pPCL had isotropic yield strains. Overall, PPCs of all modifications had elastic moduli of 3.79 ± 0.90 MPa and 0.46 ± 0.21 MPa in the parallel and perpendicular directions, respectively. Valvular interstitial cells seeded atop anisotropic aPCL displayed an actin distribution aligned in the direction of the underlying fibers. The resulting scaffold combines the biocompatibility and tunable fabrication of PEG with the strength and anisotropy of ePCL to form a foundation for future engineered valve scaffolds.

Introduction

Up to now, there has been only limited success in tissue engineering an aortic valve, the connective tissue that maintains unidirectional blood flow between the left ventricle and the systemic circulation. Previous tissue-engineered valves have generally suffered from disorganized extracellular matrix (ECM) and functional incompetence.[1–4] A common thread between these previous valves is the use of isotropic and homogenous synthetic scaffolds, which do not fully approximate valvular leaflet structure and behavior. First, the valvular leaflet is anisotropic, being stiffer in the circumferential direction than in the radial direction due to the circumferential orientation of collagen fibers.[5–7] Second, the leaflet is a laminate structure consisting of the fibrosa, spongiosa, and ventricularis layers, which are comprised of predominantly collagen, glycosaminoglycans, and elastic fibers, respectively. These properties combine to make the leaflet both flexible and strong in tension, while creating a heterogeneous mechanical environment for cells. Thus, the recapitulation of the native anisotropy and laminate structure within scaffolds for engineered valves may be a means of improving both its functionality and mechanobiology.

Toward that broad goal of an anisotropic, laminate scaffold, this study focuses on one layer of the leaflet—the fibrosa—which is the primary location of the circumferentially oriented collagen fibers that give rise to the leaflet's anisotropy and tensile strength. In this study, the anisotropy is generated through the use of a composite scaffold. The materials of interest for this scaffold are hydrogels, specifically poly(ethylene glycol) (PEG)–based hydrogels. PEG is biocompatible, can be photopolymerized under favorable conditions for cell encapsulation and functionalized with peptides to direct cellular behavior.[8–12] Most importantly for this study, PEG has tunable material properties that can approximate the different stiffnesses of the leaflet layers and can be laminated with strong interfaces.[13–15] The main obstacle to the use of a PEG hydrogel as the sole material in an engineered valve is its low strength and isotropic material behavior.[16] Given that limitation, this study augmented PEG hydrogels by embedding a second material, electrospun polycaprolactone (PCL) scaffolds, to improve strength and

[1]Department of Bioengineering, Rice University, Houston, Texas.
[2]Department of Biomedical Engineering, Duke University, Durham, North Carolina.
*These authors contributed equally to this manuscript.

introduce anisotropy. PCL is a biodegradable aliphatic polyester, with a stiffness comparable to the native valve leaflet; PCL and similar electrospun materials have been previously reported as potential scaffolds for heart valve tissue engineering.[17,18] Additionally, PCL can be fabricated into aligned, finely fibrous scaffolds through electrospinning onto a rotating collector to introduce anisotropy.[19] However, PCL scaffolds suffer from issues with cell infiltration,[20] and the hydrophobicity of PCL is a practical challenge to embedding electrospun scaffolds within an aqueous PEG hydrogel, as it requires a considerable length of time for the PEG precursor solution to soak through the PCL, limiting cell infiltration and the achievable size of the scaffold. As such, modifying the PCL before embedding must be taken into consideration.

Several previous reports describe approaches for embedding fibrous polymers within hydrogels for applications ranging from drug release to neural and bone tissue engineering.[21–27] The approach that was the most comparable to this study used unmodified electrospun poly-L-lactic acid scaffolds that were either embedded in a PEG hydrogel or were briefly soaked in PEG, and then crosslinked.[23] The addition of PEG reduced the ultimate tensile strength of the scaffold, although its strength was within a physiologically desired range.[23] Developing a composite scaffold in which PCL is embedded into PEG would generate a fibrosa-like scaffold that combines the biocompatibility and tunability of PEG hydrogels with the strength and anisotropy of PCL. In the future, this composite could be readily prepared as part of a laminate scaffold for heart valve tissue engineering.

In this study, PCL was electrospun into aligned scaffolds (ePCL) and then rendered hydrophilic in three different ways to achieve the same composite material: protein adsorption (pPCL), alkali digestion (hPCL), and acrylation (aPCL) to allow bonding between the PCL and PEG. Uniaxial tensile testing was used to determine the effect of the three different modifications on PCL strength and anisotropy. Modified PCL was embedded into PEG to form PEG-PCL composites (PPCs), which were also characterized using uniaxial tensile testing. Lastly, aortic valvular interstitial cells (VICs) were seeded atop either PEG alone or PPCs containing either isotropic or anisotropic aPCL in order to confirm that the differences in stiffness and anisotropy would be reflected by the cellular response. The result of this study was a scaffold that combines the benefits of PEG and PCL to mimic the strength, anisotropy, and laminability of the native aortic valve leaflet.

Materials and Methods

Electrospinning PCL

Electrospinning was used to fabricate fibrous PCL scaffolds. A 15% (w/v) solution of PCL ($M_w = 70$–90 kDa; Sigma-Aldrich, St. Louis, MO) was prepared in 1:1 tetrahydrofuran (Sigma-Aldrich):N,N-dimethylformamide (Sigma-Aldrich) and mixed overnight. The PCL solution was loaded into a syringe pump (Cole-Parmer, Vernon Hills, IL) and extruded from a 25 G needle at a rate of 1 mL/h. The solution was charged at the needle tip at a voltage of 12 kV using a high-voltage supply (Gamma High Voltage Research, Ormond Beach, FL) to whip and dry the PCL solution into fibers, which were then collected on a grounded collector 20 cm from the needle tip (Fig. 1B).

In this study, two types of collectors were used. First, a flat copper collector (76.2 mm width × 76.2 mm length × 6.35 mm thick, 5.81×10^3 mm^2 surface area) was used to collect randomly aligned scaffolds, which are referred to as isotropic ePCL. Scaffolds were collected on this collector at a rate of 200 μm/h. Second, a rotating mandrel was used to collect aligned scaffolds that are referred to as anisotropic ePCL. The rotating mandrel consisted of an aluminum drum (63.5 mm outer diameter × 69.85 mm length × 3.175 mm thick, 1.39×10^4 mm^2 surface area) attached to a grounded copper rod (6.35 mm outer diameter × 76.2 mm length) spinning at a rotational speed of 4000 rpm. Anisotropic ePCL was collected at a rate of 83 μm/h. In this text, the directions parallel and perpendicular to fiber alignment are analogous to the circumferential and radial directions in the leaflet. Once fabricated, all ePCL scaffolds were removed from the collector and stored in a desiccator at room temperature until further use.

Scanning electron microscopy

Scanning electron microscopy (SEM) was used to characterize ePCL. Squares (5 mm width × 5 mm length) were cut from ePCL sheets and mounted onto microscope stubs. The samples were sputter coated with gold (20 nm, Desk V Sputter Coater; Denton Vacuum, Moorestown, NJ) and imaged with an SEM (Quanta 400; FEI, Hillsboro, OR). Images were taken at 2500 × magnification with a resolution of 1024 × 768 in 8-bit grayscale. The angular distribution of ePCL scaffolds was calculated using custom image analysis software in MATLAB (Mathworks, Natick, MA).[18,28–30] Briefly, an edge-detection algorithm was used to find the fiber directions within the whole image with 11 × 11 pixel ($s = 5$) vertical and horizontal masks ($\sigma = 2.5$).[29] The gradient-weighted contribution of each pixel was then calculated for each angle, with a histogram of angular distribution for each image calculated ($n = 5$ scaffolds per group). Fiber diameters were also measured, using a method similar to a previously reported approach to assess the spacing of elastic fibers in the leaflet.[28] Images were taken at three separate locations, with the angular distributions and fiber diameters for a particular scaffold averaged from the three images.

Modification of PCL

As PCL is hydrophobic, ePCL was modified in three ways with the intent of making it hydrophilic to improve embedding within an aqueous PEG precursor solution (Fig. 2). For the first modification, pPCL was fabricated by soaking ePCL in bovine growth serum (BGS; Hyclone, Logan, UT) and shaking it on a rotary shaker at 4°C for 24 h. For the second modification, hPCL was prepared by soaking ePCL in 1 M NaOH at room temperature for 30 min to break down ester bonds on the surface of PCL fibers and expose carboxyl groups, rendering ePCL hydrophilic.

For the third modification, aPCL was prepared using an approach similar to a previously reported method modifying PCL with methacrylate groups (see Supplementary Fig. S1A for a schematic of acrylation; Supplementary Data are available online at www.liebertpub.com/tea).[31] Here, ePCL was soaked and shaken on a rotary shaker in 1 M ammonium persulfate for 90 min at room temperature and then 1 M sodium hydroxide for 30 min at room temperature, with a

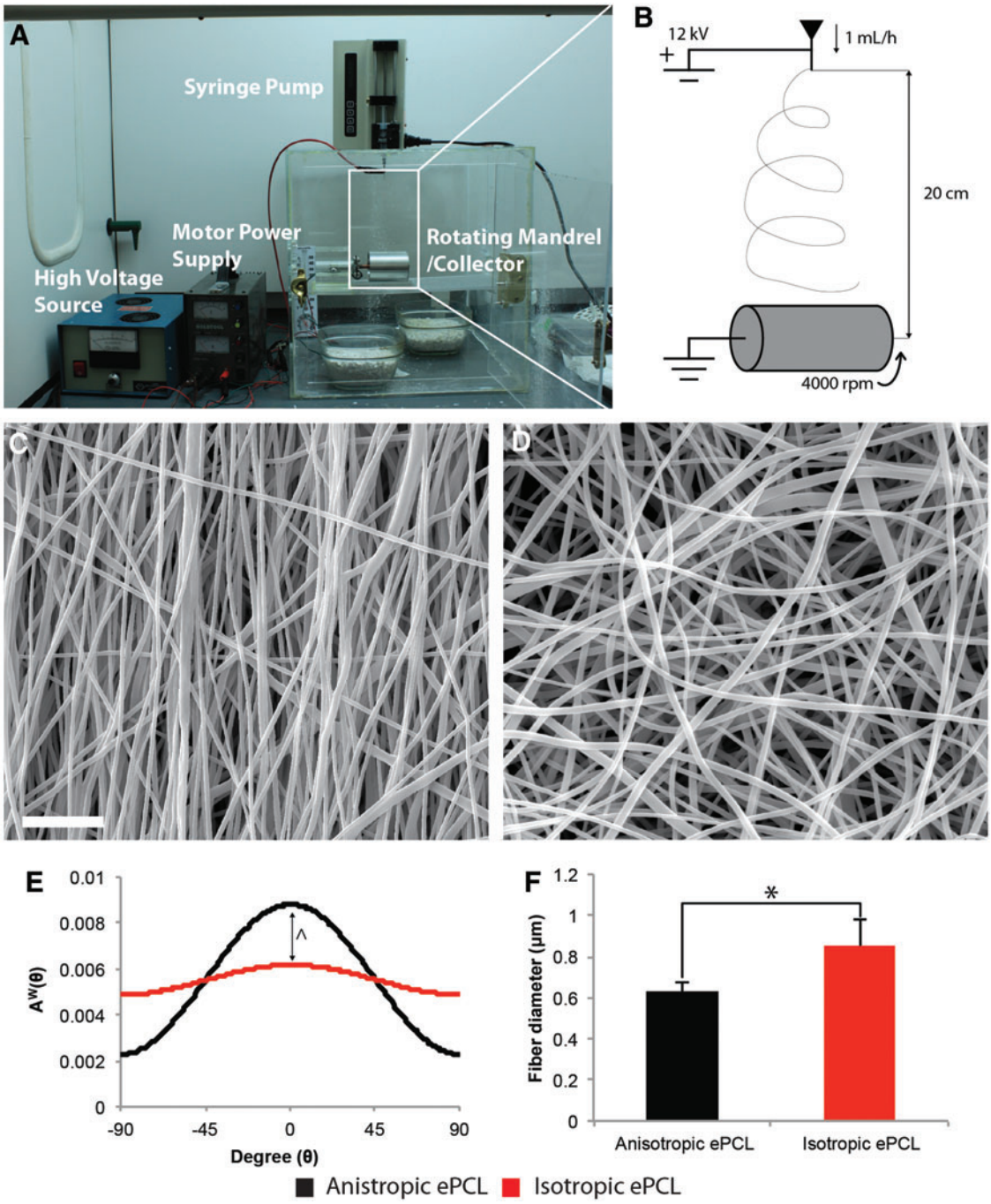

FIG. 1. The **(A)** electrospinner and **(B)** a schematic of the electrospinning process and its parameters. Polycaprolactone (PCL) solution was extruded out of a syringe at 1 mL/h and charged at 12 kV to spin a fibrous matrix onto a collector 20 cm from the needle tip. ePCL was collected on either a flat collector (isotropic) or a rotating mandrel (anisotropic). Scanning electron microscopy (SEM) micrographs of **(C)** anisotropic and **(D)** isotropic scaffolds show a stark difference in orientation between the two groups. Scale bar = 10 μm. **(E)** The orientation of fibers was confirmed using image analysis, with PCL fibers in anisotropic ePCL (black) demonstrating a significantly different distribution with a dominant orientation in comparison to those isotropic ePCL (red). $^{p} < 0.001$ between curves. **(F)** There was also a significant difference in fiber diameter between anisotropic and isotropic ePCL. $^{*}p < 0.05$ within bracket. Error bars represent standard deviation. Color images available online at www.liebertpub.com/tea

wash in ethanol in between, to render the scaffold hydrophilic and expose carboxyl groups. Next, the scaffolds were washed in 0.1 M 2-(N-morpholino)ethanesulfonic acid hydrate (MES, pH = 6.0; Sigma-Aldrich) buffer, and mixed with 5 mM 1-ethyl-3-[3-dimethylaminopropyl]carbodiimide hydrochloride (EDC; Thermo Scientific, Rockford, IL) and 10 mM N-hydroxysuccinimide (NHS; Thermo Scientific) in MES buffer for 30 min to convert carboxyl groups to amine reactive NHS-ester groups. After washing with MES buffer (pH = 7.0 from this step onward), the scaffolds were soaked

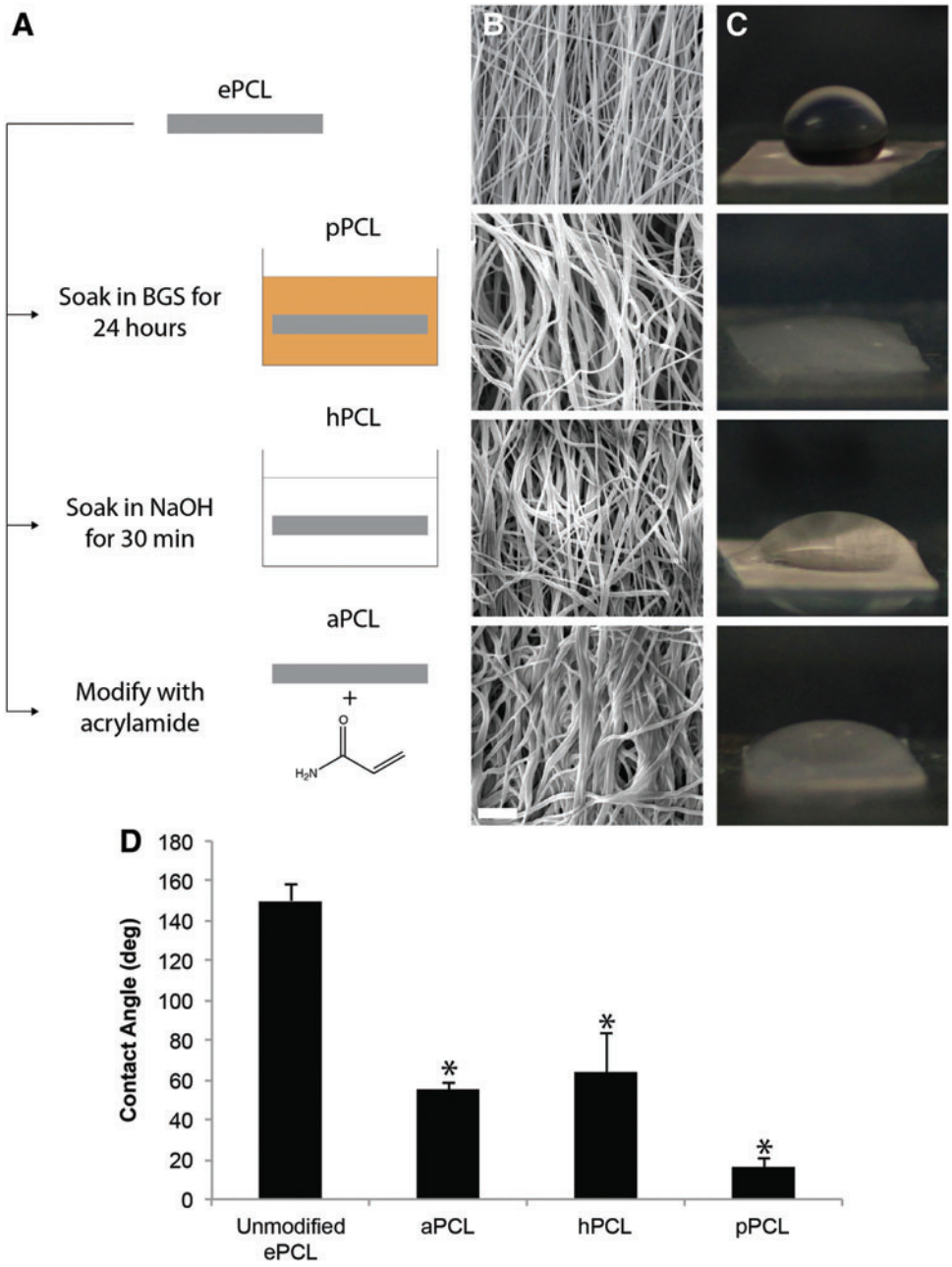

FIG. 2. **(A)** ePCL was modified in three ways to embed in poly(ethylene glycol) (PEG): by soaking in bovine growth serum (BGS) (pPCL), by soaking in NaOH (hPCL), and by acrylation (aPCL). **(B)** SEM micrographs of the modified anisotropic ePCL demonstrated that fiber alignment was generally maintained. Note the increase in thickness of fibers as a result of protein adsorption in pPCL, and the wider angular distribution of fibers in aPCL. Scale bar = 10 μm. **(C)** Modified ePCL was more hydrophilic than unmodified ePCL as shown by the contact angle of 25 μL droplets on the PCL. The contact angles of modified ePCL **(D)** were all significantly lower than that of unmodified ePCL. $*p < 0.01$ versus unmodified ePCL. Color images available online at www.liebertpub.com/tea

and shaken on a rotary shaker with 50 mM acrylamide (Sigma-Aldrich) in MES buffer to react and convert NHS-esters to acrylate groups. Finally, after washing with MES buffer, the scaffold was soaked in 50 mM Tris (MP Biomedicals, Santa Ana, CA) in ultrapure H_2O to react any leftover NHS-ester. Acrylation was verified by the binding of fluorescently tagged PEG-thiol (see Supplementary Fig. S1B–C and Verification of Acrylation in Supplementary Data). All modified scaffolds were lyophilized and stored in a desiccator until further use.

To verify the hydrophilicity as a result of the modifications, the contact angles of water droplets on each modified PCL were measured. Modified ePCL of thickness 125 μm was cut into $5 \times 5\ mm^2$ squares and attached to a glass slide using double-sided tape. A droplet of 25 μL of ultrapure H_2O was added to each square, and the angle between the bottom surface and the droplet was measured ($n = 3$ per modification).

Hydrogel synthesis

PEG-diacrylate (PEGDA) was synthesized as previously described.[32] Dry PEG (either 3.4 or 6 kDa, Sigma-Aldrich) was dissolved in anhydrous dichloromethane to a concentration of 1 M. Triethylamine (Sigma-Aldrich) and acryloyl chloride (Sigma-Aldrich) were added to the solutions at 2:1 and 4:1 molar ratios, respectively, to react overnight. The resulting solution was next washed with 1 M K_2CO_3 and phase separated overnight, after which the organic phase was dried using anhydrous $MgSO_4$ and filtered. The filtered solution was then precipitated in diethyl ether,

filtered, lyophilized, finely ground into powder, and finally stored at −20°C until further use. Acrylation was verified with proton nuclear magnetic resonance (^{1}H-NMR) spectroscopy.

PEG was also conjugated to the adhesive cell-peptide sequence RGDS (PEG-RGDS) as previously described.[33] RGDS (American Peptide, Sunnyvale, CA) was reacted with monoacrylate PEG-succinimidyl valerate (Laysan Bio, Arab, AL) at a 1.2:1 molar ratio in phosphate-buffered saline (PBS) overnight and then dialyzed against ultrapure H_2O at room temperature for 2 days with multiple changes. The subsequent solutions were lyophilized and stored at −20°C until further use. The peptide conjugation was verified with gel permeation chromatography.

To prepare the hydrogels, prepolymer solutions with the desired molecular weight and concentration of PEGDA were mixed with 5 mM PEG-RGDS in ultrapure H_2O. Irgacure 2959 (I2959, 100 mg/mL in ethanol; Sigma-Aldrich) was next added to reach a final concentration of 0.3%. The prepolymer solution was then mixed and poured into a 250 μm thick mold between two glass slides coated with Sigmacote (Sigma-Aldrich). The molds were exposed to ultraviolet light (365 nm, 10 mW/cm^2) for 10 min, with the molds turned over after 5 min. The resulting gel was removed from the mold and swelled in PBS for at least 24 h before use.

PEGDA-PCL composite fabrication

After modification, ePCL scaffolds were embedded in PEGDA to form PPCs. ePCL scaffolds of 125 μm thickness were fabricated and modified as described previously. Modified ePCL scaffolds were placed in a mold consisting of a 250 μm thick silicone spacer sandwiched between two glass slides coated with Sigmacote. A prepolymer solution consisting of 10% (w/v) 3.4 kDa PEGDA, 5 mM PEG-RGDS, and 0.3% I2959 was then poured into the mold. The prepolymer solution was allowed to soak into the modified ePCL for 5 min. Once fully soaked, the molds were exposed to UV light (365 nm, 10 mW/cm^2) for 10 min, with the molds turned over after 5 min. The resulting gel was removed from the mold and swelled in PBS at least 24 h.

PPCs were imaged with SEM under similar conditions to ePCL. 250 μm thick PPCs containing 125 μm thick aPCL scaffolds were lyophilized and then either mounted whole onto an SEM stub to view its surface, or finely sectioned with a scalpel (~1 mm thick) to expose its cross-section and then mounted onto an SEM stub with its cross-section facing upward. The PPCs were finally sputter coated and imaged as previously described for ePCL scaffolds.

Cryosectioning

PPCs were sectioned to view the specimens in cross-section. PPCs were soaked overnight in a solution of 30% (w/v) sucrose in ultrapure H_2O and then soaked in a support medium (Tissue-Tek OCT; Sakura Finetek, Torrance, CA) for 24 h. The pieces were then flash frozen in liquid N_2 and sectioned into 30 μm thick sections using a cryostat (Leica CM1850UV; Leica Microsystems, Buffalo Grove, IL). The sections were finally imaged on an upright microscope (Leica DM LS2; Leica Microsystems).

Mechanical testing

All samples were tested in a uniaxial tensile tester (ELF 3200; Bose Electroforce, Eden Prairie, MN) with a 1000 g load cell (Bose Electroforce). The samples were tested in the directions parallel and perpendicular to fiber alignment ($n = 5$ scaffolds/gel per direction per group, three replicates per scaffold/gel), which are analogous to the circumferential and radial directions on the valve, respectively. In the cases of isotropic ePCL and PEG gels, samples were tested in two orthogonal directions, with the directions arbitrarily designated as parallel and perpendicular. Samples were cut in 5 mm wide × 30 mm long strips for testing. Each sample type was gripped differently. Hydrogels were gripped by gluing pieces of paper to both sides of the gel on both ends, which were gripped during testing.[13] ePCL was gripped directly with fine sandpaper (grit size = 600). PPCs were also gripped directly with fine sandpaper, with the swelling pressure created between the PCL and PEG resisting compression of the hydrogel. Before testing, the thicknesses of the samples were measured under a stereo microscope (MZ6; Leica Microsystems, Wetzlar, Germany). The original gage length and width of the sample were measured after the sample was loaded in the tester, but prior to testing. Samples were pulled at a displacement rate of 1 mm/s for a total of 10 mm, with load and displacement gathered at a sampling rate of 100 points/s.

The data were analyzed using custom software coded in MATLAB (Fig. 3). After conversion from load and displacement to stress and strain, the yield point of the stress–strain curve was found by performing a linear least-squares fit between zero strain and any point between 10% and 100% total strain that yielded the highest r^2. The yield strain (ε_y), and the elastic modulus (E), which was found as the slope of the linear fit, were recorded.

Cell culture

VICs were chosen for use in this study because they are the main constituent cell type of the valve leaflet. Since VICs demonstrate phenotypic characteristics of fibroblasts and smooth muscle cells,[34] results from VIC studies such as

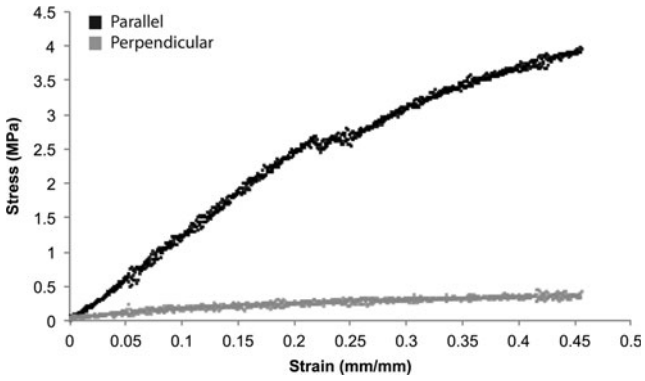

FIG. 3. Representative stress–strain (σ–ε) curves of unmodified anisotropic ePCL in the directions parallel (black) and perpendicular (gray) to the fiber alignment. These directions relate to the circumferential and radial directions, respectively, in the native aortic valve leaflet. Anisotropic ePCL was stiffer in the parallel direction than in the perpendicular direction.

this work can potentially be translated to nonvalve cell sources that are more clinically feasible for the development of tissue-engineered heart valves. VICs were harvested from fresh porcine aortic valve leaflets from a commercial abattoir (Fisher Ham and Meats, Spring, TX) using a two-step collagenase digestion consisting of collagenase type II (450 U/mL; Worthington Biochemical, Lakewood, NJ), collagenase type III (350 U/mL; Worthington Biochemical), and hyaluronidase (50 U/mL, bovine testicular; Worthington Biochemical).[35] VICs were cultured in Dulbecco's modified Eagle's medium/F12 medium supplemented with 10% BGS, 1% 4-(2-hydroxyethyl)-1-piperazineethanesulfonic acid (HEPES) buffer, and 1% penicillin-streptomycin and maintained in a humidified environment (37°C, 5% CO_2, 95% humidity). VICs were used following their third passage.

Cytoskeletal staining of VICs on PPCs

VICs were seeded atop PPCs in order to view the cytoskeletal and adhesive response to the anisotropy and high stiffness of the PPC versus PEG alone (Fig. 7A). PPCs were prepared by embedding a 5 mm wide × 5 mm long × 250 μm thick aPCL square within a 10% (w/v) 6 kDa PEGDA hydrogel containing 5 mM PEG-RGDS. 6 kDa PEG was used for these cellular response studies because, since the higher molecular weight produces a softer gel, stark contrasts in adhesion between the PPC and PEG would be shown. aPCL, which was prepared using both anisotropic and isotropic ePCL, was used as the representative modified ePCL for these studies. aPCL was selected since the PEG prepolymer solution appeared to wick rapidly through this particular scaffold, although the results of this experiment are not considered to be modification dependent and could be extended to the other types. PPCs were fabricated under sterile conditions in a 5 mm wide × 10 mm long × 250 μm thick mold between two glass slides coated with Sigmacote. Within the mold, the aPCL was placed to one side, leaving the other half empty. After adding PEG, the resulting gel was a continuous piece consisting of PPC on one side and PEG on the other side of the same gel. This method was used to ensure direct comparisons of the VIC response between the two substrates on the same sample. The bottom surfaces of the hydrogels were crosslinked to methacrylated glass coverslips to weigh down the gels in cell culture plates.[36] After fabrication, the gels were placed in 24-well plates and sterilized under UV overnight while swelling in PBS. The next day, the PBS was replaced with media and the gel was left to swell for another 4 h. The media was removed and VICs were seeded on the gels at a concentration of 50,000 cells/well. After 36 h of culture, the media was aspirated and the gels were fixed in 4% paraformaldehyde for at least 15 min.

These cells were stained for F-actin with fluorescently labeled phalloidin (1:40 in PBS, AlexaFluor 488; Invitrogen, Carlsbad, CA) and counterstained for nuclei with 4′,6-diamidino-2-phenylindole (1:1000, DAPI; KPL, Gaithersburg, MD) for 2 h at room temperature. The gels were rinsed thoroughly and imaged on a confocal microscope (LSM 5 LIVE; Zeiss, Jena, Germany). Image analysis was performed on the resulting images, using ImageJ (NIH, Bethesda, MD) and MATLAB ($n = 2$–3 scaffolds per group). The angular distribution of actin was calculated in MATLAB using the same method as described for finding the angular fiber distribution of ePCL scaffolds.[18,28–30] ImageJ was used to determine the nuclear aspect ratios of the cells.

Statistical analysis

All data were analyzed using statistical analysis software (SigmaStat; Systat Software, San Jose, CA). Significance was defined as $p < 0.05$. One-way ANOVAs were performed to compare the fiber diameters between anisotropic and isotropic ePCL, and the differences in nuclear aspect ratio and area among cells seeded on anisotropic PPC, isotropic PPC, and PEG. Two-way ANOVAs were performed on the mechanical testing data to compare the effects of modification treatment as well as between the directions parallel and perpendicular to the predominant fiber direction. If an overall effect was found in the ANOVAs, then *post hoc* Tukey's testing was performed to observe comparisons between groups. For the effect of alignment on PCL fiber distribution, and the effect of substrate on VIC actin alignment, the sample variances were compared using an F-test. All values are presented as mean ± standard deviation.

Results

Electrospinning

PCL was successfully electrospun into anisotropic and isotropic scaffolds on a rotating mandrel and flat collector, respectively. As demonstrated by SEM, there was a stark difference in fiber alignment between the two ePCL scaffolds. Fibers were predominantly aligned in one direction in anisotropic ePCL (Fig. 1C), while randomly oriented in isotropic ePCL (Fig. 1D). This observation was verified by analysis of the angular distributions of PCL fibers, as anisotropic ePCL was found to be significantly more aligned compared with isotropic ePCL (Fig. 1E, $p < 0.001$). The diameters of PCL fibers were found to be significantly greater in isotropic ePCL than in anisotropic ePCL (Fig. 1F, $p < 0.05$).

PCL modification

When viewed under SEM, the fiber alignment in the three types of modified ePCL was generally maintained. In pPCL scaffolds, protein adsorption resulted in thicker fibers (Fig. 2B) compared with the unmodified ePCL. In aPCL scaffolds, fibers appeared to be more randomly oriented than in the unmodified ePCL. hPCL generally appeared to be unaffected by treatment. Modified ePCL was also shown to be hydrophilic through measurements of contact angles of 25 μL H_2O droplets (Fig. 2C). All modifications resulted in significantly reduced contact angles compared with unmodified ePCL (Fig. 2D, $p < 0.01$). Consequently, in all three cases, the PEG prepolymer solution was able to soak quickly through the modified ePCL. PPCs were successfully formed with ePCL scaffolds prepared using any of the three modifications studied.

In terms of mechanical properties, unmodified anisotropic ePCL had a higher E in the parallel direction (Fig. 4A, $p < 0.001$) and had a higher ε_y in the perpendicular direction (Fig. 4B, $p < 0.001$). Isotropic ePCL had statistically similar values for E and ε_y regardless of direction. The modified ePCL scaffolds maintained the anisotropy of the ePCL, being significantly stiffer in the parallel direction compared with the perpendicular direction ($p < 0.05$). In the parallel

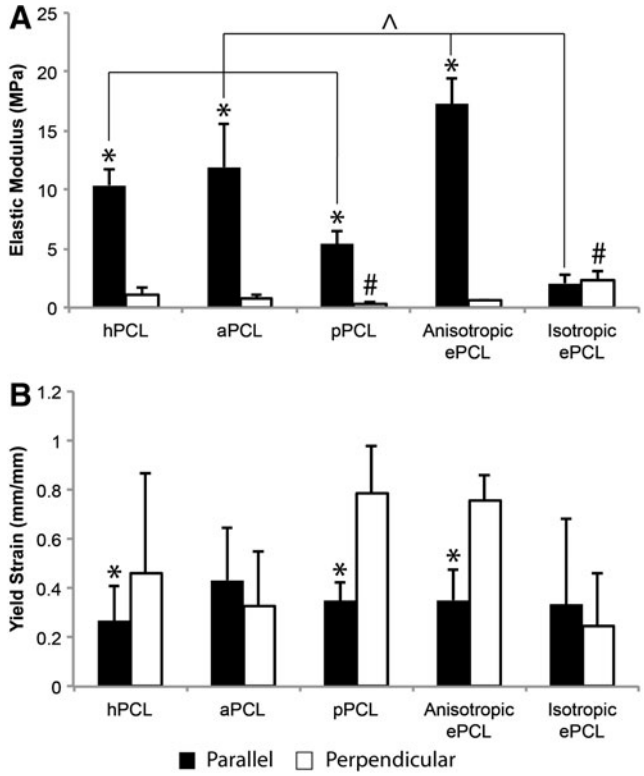

FIG. 4. **(A)** Elastic modulus (E) and **(B)** yield strain (ε_y) of modified ePCL scaffolds and unmodified anisotropic and isotropic ePCL scaffolds in the parallel (black) and perpendicular (white) directions. All modified ePCL was stiffer in the parallel direction than in the perpendicular direction (as were the anisotropic ePCL scaffolds) and underwent greater strain to failure in the perpendicular direction, except for aPCL. E generally did not decrease in the perpendicular direction, with only pPCL having a significantly lower E than isotropic ePCL. $^{*}p<0.05$ versus perpendicular direction, $^{\wedge}p<0.05$ within bracket, $^{\#}p<0.05$ between pairs. Error bars represent standard deviation.

direction, the modified ePCL all had significantly lower E compared with unmodified anisotropic ePCL ($p<0.05$). There was no difference in perpendicular E between modified PCL and unmodified anisotropic ePCL, although the pPCL was significantly less stiff in the perpendicular direction than was the isotropic ePCL ($p<0.02$). With regards to ε_y, both hPCL and pPCL maintained the anisotropic yield behavior of the unmodified anisotropic ePCL ($p<0.05$), but the yield strains of aPCL were not significantly different between directions.

PPC fabrication

SEM micrographs (Fig. 5B) and cryosections (Fig. 5C) of the PPC in cross-section demonstrated that the modified PCL was thoroughly embedded within the PEG gel. The surface of the PPC appears to be dense and uniform from the PEG with negligible effect on the topography from the underlying PCL (Fig. 5D).

The results of tensile testing of PPCs showed that PPCs maintained the anisotropy of the elastic modulus (Fig. 6A, $p<0.001$) that was characteristic of the unmodified anisotropic ePCL, although the E in the parallel direction was significantly reduced ($p<0.05$). There was no significant difference in E among the PPC types in either of the directions. Overall, PPCs had an E of 3.79 ± 0.90 MPa in the parallel direction and 0.46 ± 0.21 MPa in the perpendicular direction. With regards to yield strain, PPCs containing hPCL maintained the anisotropic ε_y of unmodified ePCL (Fig. 6B, $p<0.001$), whereas PPCs containing aPCL and pPCL did not show anisotropic yield strain behavior. As expected, the E and ε_y of PEG did not vary with direction.

VIC morphology on PPCs

Staining with DAPI and phalloidin demonstrated that VICs grown atop PPCs had a more spread morphology compared with VICs grown atop PEG alone (Fig. 7B). It was also evident from comparisons of VICs seeded on anisotropic and isotropic PPCs that the VICs demonstrated an alignment of actin matching the fiber orientation of the underlying aPCL. Image analysis of the angular distribution of actin demonstrated that VICs grown atop anisotropic PPCs had an angular fiber distribution that was significantly narrower (more aligned) than the VICs grown atop the isotropic PPCs or PEG alone (Fig. 7C, $p<0.002$). There was no significant variation in nuclear aspect ratio between the different substrates (Fig. 7D).

Discussion

In this study, an anisotropic composite scaffold (PPC) consisting of PEG and PCL was designed, fabricated, and mechanically characterized for the purpose of heart valve tissue engineering. PCL was electrospun and then chemically modified in order to allow rapid embedding of the scaffold within an aqueous PEG hydrogel, which increased the overall scaffold strength and imparted anisotropic mechanical behavior. PCL was modified in three ways: by protein adsorption (pPCL), by treatment with NaOH (hPCL), and by acrylation (aPCL). Tensile testing of modified ePCL demonstrated that all modifications maintained anisotropy of their elastic modulus. Both pPCL and hPCL maintained anisotropic yield strain. The anisotropy of the elastic modulus was still preserved even after embedding the modified ePCLs into PEG hydrogels to generate PPCs. VICs seeded on PPCs containing anisotropic aPCL showed an aligned orientation of actin compared with VICs seeded on PPCs containing isotropic aPCL or seeded on PEG alone. Importantly, the VICs were influenced by the presence and fiber alignment of the encapsulated ePCL even though they were not seeded directly atop the ePCL. Overall, this study combined both PEG and PCL to generate a scaffold with elastic moduli and degrees of anisotropy that were comparable to the native aortic valve leaflet. Along with previous work on laminate and cell-encapsulated hydrogels,[13,37] this study offers a basis for preparation of a laminate composite hydrogel scaffold for heart valve tissue engineering. The results of this study can also apply to other engineered tissues of interest in which lamination and anisotropy are key features to recapitulate, such as blood vessels, intervertebral discs, and tendons.

This study demonstrated that three different methods to modify the ePCL promoted rapid encapsulation of the ePCL within the PEG prepolymer solution. Although several

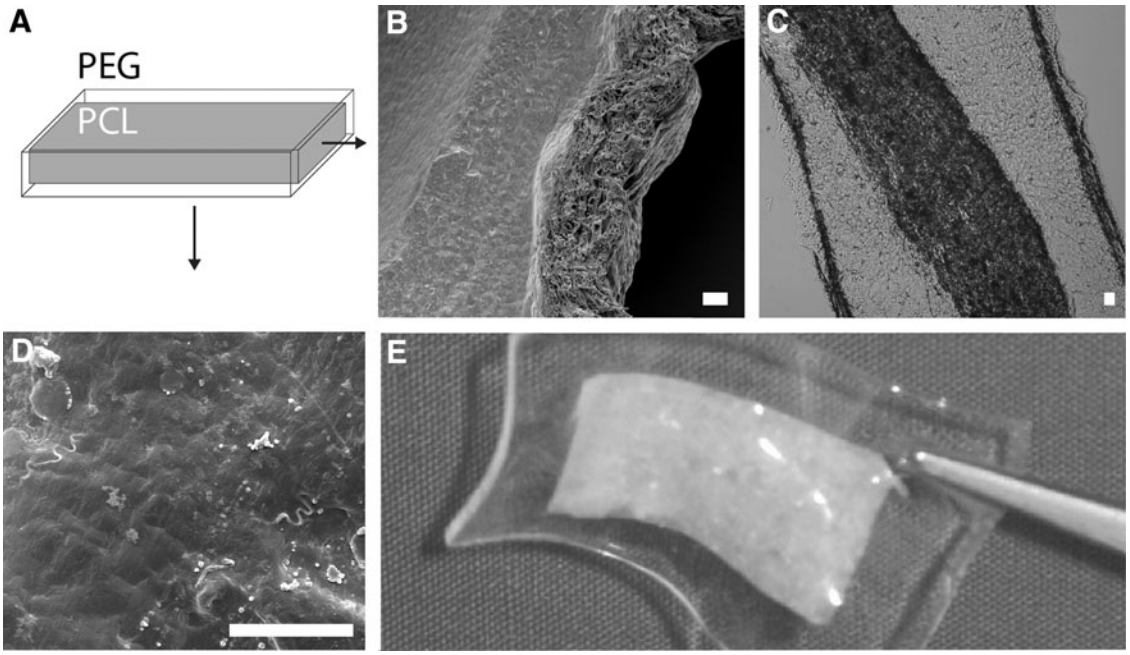

FIG. 5. **(A)** Schematic of the PEG-PCL composites (PPC), with the modified PCL embedded within the PEG hydrogel. The cross-section of a 500 μm PPC embedded with 250 μm aPCL as shown by **(B)** SEM micrograph and **(C)** image of a cryosection. The aPCL is seen to be fully embedded within the PEG hydrogel. An SEM micrograph of the surface of the same PPC **(D)** showed a dense, uniform topography, and no visible orientation as a result of the embedded aPCL. Scale bar = 20 μm. **(E)** PPC containing embedded aPCL.

previous studies have reported embedding unmodified PCL into PEG,[21–26] the modification of ePCL that was performed in this work significantly reduced the fabrication time of the PPC. hPCL was the simplest modification, in which hydrophilicity was introduced using alkali digestion.[38–41] The pPCL was tested to mimic simple protein adsorption to the PCL. The third modification strategy, aPCL, was performed in order to covalently bind the PCL to the PEG within the PPC. Although acrylation was the most extensive of the three modifications in terms of preparation, the PEG prepolymer solution wicked into the aPCL more rapidly than it did for the other two types. Even though all modification types generally maintained the anisotropy of the ePCL, the most apparent advantage of acrylation would be that such binding would improve long-term mechanical properties by effectively distributing stress across the scaffold. PEG-PCL binding in the aPCL could be finely controlled by varying the molarities of EDC, NHS, or acrylamide, as well as the reaction times. It was noted, however, that acrylation resulted in the loss of anisotropy of yield strain, possibly due to the loss of angular fiber distribution that was seen in the aPCL. Further, in the short term, the mechanical performances of pPCL and hPCL were comparable to aPCL. pPCL was fabricated using serum to mimic protein adsorption, but could be implemented with a specific protein of interest to drive scaffold remodeling, although the necessary amount of protein and adsorption time could be limiting factors. It is also worth discussing the issue of slip between the PCL and PEG scaffolds. As noted earlier, acrylation was used to bind the PCL and PEG and thus promote stress distribution. On the other hand, the alkali digestion and protein adsorption strategies could have slip the between PEG and PCL, which could improve long-term scaffold performance by shielding the hydrogel and encapsulated cells from high stress when there is active deformation of the combined PPC, such as in diastole. Slip between these two surfaces could also increase the extensibility of the combined scaffold, although no difference in extensibility was found between aPCL and pPCL. Overall, the results of this study demonstrate the need for further investigation of the effects of these modifications on scaffold mechanical behavior and eventual cell remodeling.

When compared to the native aortic valve leaflet, the elastic moduli of the PPCs ($E_{para} = 3.79 \pm 0.90$ MPa, $E_{perp} = 0.46 \pm 0.21$ MPa over all modification types) compared favorably to the elastic moduli of the leaflet, which has been reported to range from 3.39–28 MPa circumferentially to 1.09–2.86 MPa radially.[5,6] A recent report from our group, performed using similar methodologies and the same mechanical tester as in this study, determined the elastic moduli of aortic valve leaflets to be 5.6 MPa in the circumferential direction and 1.5 MPa in the radial direction.[42] The elastic moduli reported for the collagenous fibrosa layer, which is primarily responsible for leaflet stiff and strength, range from 13–23 MPa circumferentially to 3.71–4.56 MPa radially.[43,44] The anisotropic ratio of the PPC elastic moduli ($E_{para}/E_{perp} = 8.22$) could be optimized by changing the rotation speed of the mandrel, as has been demonstrated in previous reports.[18] While similar in elastic modulus, there were still stark differences in stress–strain behavior between PPCs and the native leaflet; the native leaflet is bilinear and elastic,[5–7] whereas the PPC has a linear stress–strain behavior, and yielded isotropically at high strains, possibly a result of embedding anisotropic ePCL in isotropic PEG. The

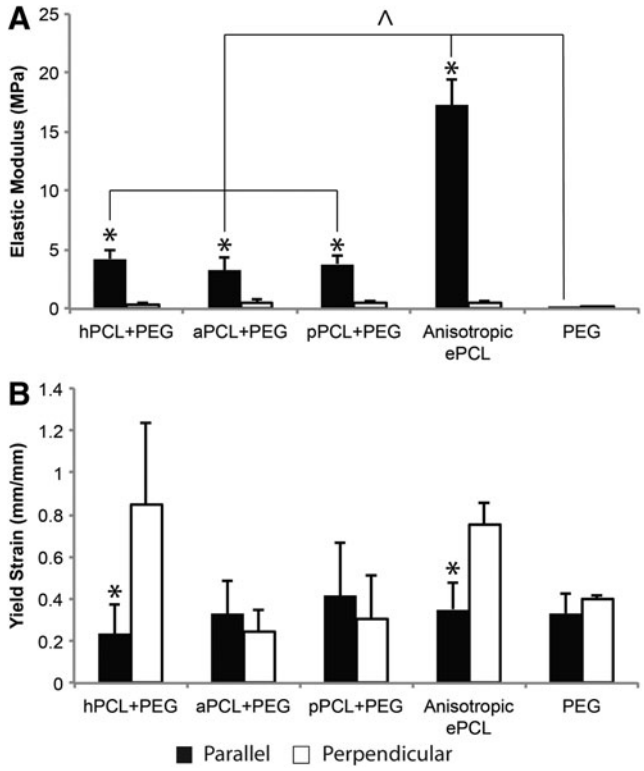

FIG. 6. **(A)** Elastic modulus (E) and **(B)** yield strain (ε_y) of PPCs with different modifications, unmodified anisotropic ePCL scaffolds, and PEG in the parallel (black) and perpendicular (white) directions. All PPC types maintained anisotropy, but had a significantly lower E in the parallel direction, and were statistically similar across all groups. aPCL and pPCL had isotropic ε_y as opposed to the ePCL, which had anisotropic ε_y. $^*p < 0.05$ versus perpendicular direction, $\wedge p < 0.05$ within bracket. Error bars represent standard deviation.

difference in behavior could present a challenge to the use of the PPC as part of a scaffold for heart valve tissue engineering. From a mechanobiology standpoint, VICs encapsulated within a scaffold with linearly elastic stress–strain behavior would experience greater stresses at low strain than they would in the native leaflet, due to the ''toe region'' of the native bilinear stress–strain curve. This linearly elastic behavior is thus a concern for any tissue-engineered valve, as high stresses are associated with VIC activation and altered ECM remodeling that can lead to calcification of native aortic valves.[45–49] Additionally, assuming the degradation of the PCL over 30 months[50] and a heart rate of 60 bpm, the scaffold would be pulled in diastole $\sim 10^7$ times. How the mechanical behavior of the study changes over these cycles, and how cells respond to these changes are key questions to answer in future studies. Thus, it will be important to examine the effects of dynamic, linearly elastic stress–strain behavior on scaffold remodeling by VICs and the long-term mechanical performance of the scaffold, and to pursue various strategies for achieving nonlinear elastic behavior.

VICs seeded atop the PPCs reinforced with aPCL showed differences in morphology and spreading compared with those grown on the other side of the same gel, where there was no PPC reinforcement. As expected, cells spread more on the stiffer PPC, confirming previous results in the literature that stiffer substrates correlate with stress fiber formation in VICs.[45] On PPCs containing anisotropic aPCL, the VICs showed predominant cytoskeletal organization in the direction of the underlying fiber alignment, demonstrating that VICs were responding to the stiffness and anisotropy of the underlying PCL within the PPC. This theory is supported by the fact that the SEM micrographs demonstrated that the surface of the PPC did not mimic the topography of the underlying PCL. It should be noted that this VIC experiment was limited to a proof of concept; the ultimate goal would be to encapsulate VICs within the hydrogel of the PPC. Cells can be encapsulated within PEG hydrogels under favorable conditions for cells[8] and with minimal effect on hydrogel lamination,[13] although cell encapsulation and the inclusion of necessary degradable peptide sequences would likely reduce the overall stiffness.[13,37,51] The finding that VICs responded to the underlying anisotropy suggests their potential to remodel the scaffold in a directional manner, which has been demonstrated previously with fibroblasts and VICs.[52,53] Further research will be required to understand the effect of cell encapsulation and material characteristics like anisotropy on scaffold remodeling.

The overall intent of this study was to prepare a composite scaffold design that mimicked the mechanical properties of the valve leaflet fibrosa layer, and would also be suitable for serving as a layer within an overall trilaminate scaffold. Other laminate scaffolds have been previously reported; one previous study designed a laminate scaffold for an engineered valve using decellularized pericardium to mimic the two outer layers, and a spongiosa scaffold derived from decellularized pulmonary arteries, within which cells were viable after 8 days in a bioreactor and stained positive for vimentin,[54] while another study used PEGDA layers supplemented with alginate that were viable after 21 days.[15] The main benefit of a laminate scaffold designed on a PEG hydrogel platform is that layers of varying functionalization and mechanical stiffness can be fabricated in a straightforward manner with strong adhesions between layers.[13] With the creation of hydrogel analogs that match the properties of the spongiosa and ventricularis, a laminate hydrogel scaffold could be fabricated using a modular assembly process. One possible approach for fabrication would be first to electrospin and modify ePCL before cutting the scaffold into leaflet shapes, which could then be placed in a mold in the shape of the aortic root. A hydrogel prepolymer solution could be added to the mold to embed the ePCL in a cellularized hydrogel of the whole aortic root, and then the other hydrogel layer analogs of the valve scaffold could be added sequentially to form a laminated engineered aortic root-valve construct. A similar fabrication strategy has previously been implemented to print aortic roots using PEGDA hydrogels.[15] The next required steps in this process will be to design hydrogel analogs for the other two leaflet layers, and develop and optimize a fabrication process for a trilaminate scaffold.

Conclusions

In this study, hydrogel-fiber composites of PEG and modified PCL were designed to combine the strength and anisotropy of electrospun PCL with the biofunctionality, tunability, and laminability of hydrogels as an analog to the

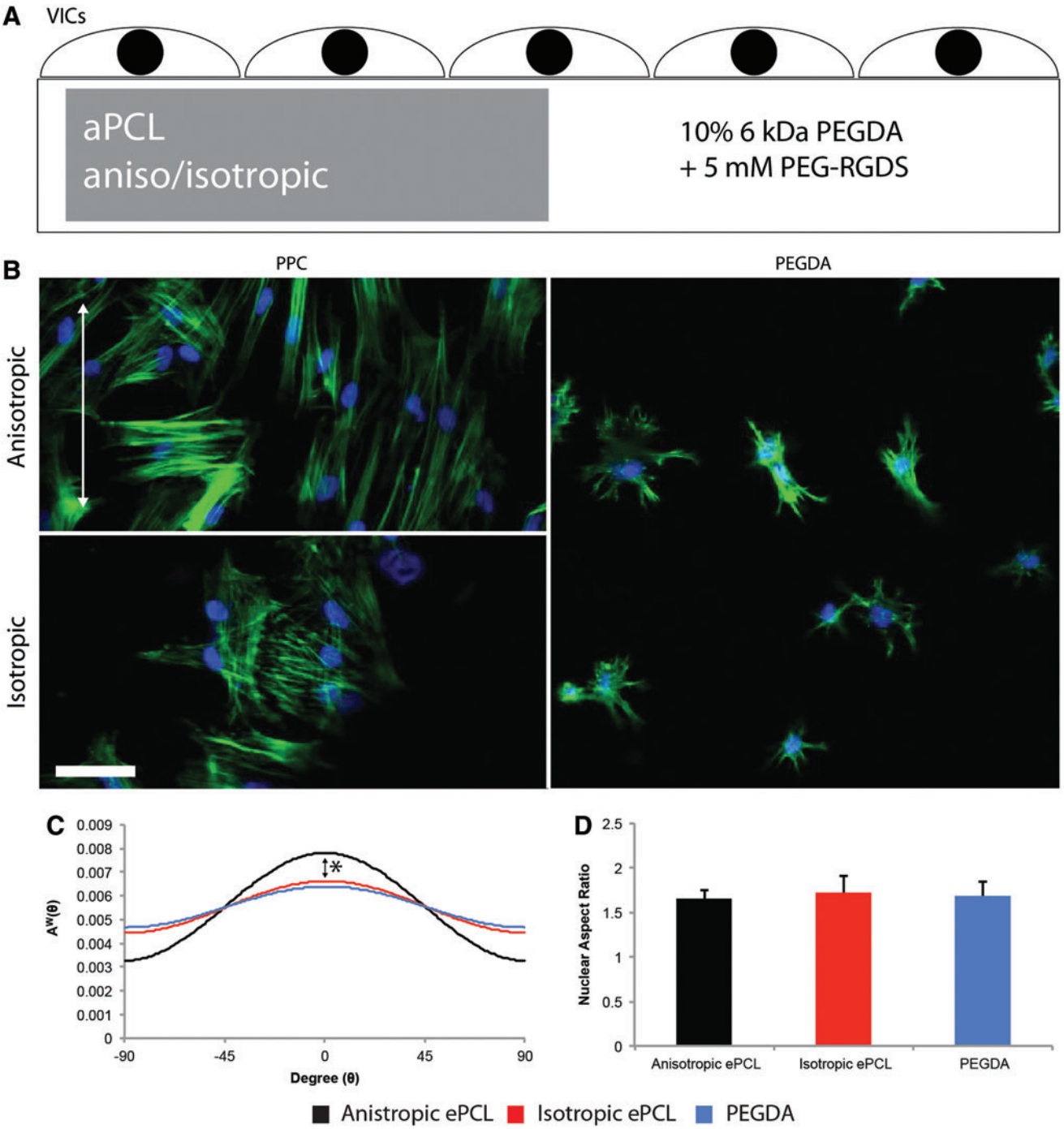

FIG. 7. **(A)** Schematic of PPCs fabricated to investigate the effect of the PPC on valvular interstitial cell (VIC) morphology. Within a 5 mm wide × 10 mm long × 250 μm thick mold, an aPCL scaffold, either anisotropic or isotropic and measuring 5 mm wide × 5 mm long × 250 μm thick, was embedded in 10% 6 kDa PEG-diacrylate (PEGDA) and 5 mM PEG-RGDS. The resulting scaffold was PPC on one side, PEG alone on the other, and contiguous throughout. Cells were then seeded on top of the scaffold. **(B)** DAPI (blue) and phalloidin (green) stains of VICs on PPCs with either anisotropic (alignment indicated by white arrow) or isotropic aPCL and on PEG. Note the spread morphology of VICs on PPCs with the stiffer aPCL compared to PEG. The alignment of actin in VICs seeded on anisotropic PPC had a dominant orientation compared with those seeded on isotropic PPC. Scale bar = 50 μm. **(C)** Actin alignment for VICs seeded on PPC with anisotropic (black) or isotropic (red) aPCL and PEG (blue). Note the difference in alignment between VICs seeded on anisotropic PPCs and the other substrates. $*p < 0.002$ anisotropic PPC versus the other groups. **(D)** There was no significant difference in nuclear aspect ratios of VICs between the substrates. Color images available online at www.liebertpub.com/tea

fibrosa layer of heart valve leaflets. Modification of ePCL via protein adsorption, NaOH treatment, and acrylation rendered the ePCL hydrophilic to facilitate embedding in PEG, and did not grossly affect the anisotropy of the ePCL. VICs seeded on top of PPCs responded to the underlying anisotropy by aligning in the prominent direction of fibers in the ePCL. The result is a scaffold that matches the anisotropy of the native aortic valve leaflet and fits well within the ideal of a modularly assembled laminate scaffold for heart valve tissue engineering.

Acknowledgments

The work in this study was supported by a predoctoral fellowship to Hubert Tseng from the American Heart Association South Central Affiliate, a graduate research fellowship to Daniel Puperi from the National Science Foundation, and a grant from the National Institutes of Health (R01HL107765). The authors thank Clark Needham, Erica Levorson, and Richard Thibault, Rice University, for their assistance with electrospinning, and Liezl Balaoing, Rice University, for the PEG-thiol used to verify acrylation.

Disclosure Statement

No competing financial interests exist.

References

1. Sodian, R., Sperling, J.S., Martin, D.P., Egozy, A., Stock, U.A., Mayer, Jr., J.E., and Vacanti, J.P. Fabrication of a trileaflet heart valve scaffold from a polyhydroxyalkanoate biopolyester for use in tissue engineering. Tissue Eng **6,** 183, 2000.
2. Sodian, R., Hoerstrup, S.P., Sperling, J.S., Daebritz, S.H., Martin, D.P., Schoen, F.J., Vacanti, J.P., and Mayer, Jr., J.E. Tissue engineering of heart valves: *in vitro* experiences. Ann Thorac Surg **70,** 140, 2000.
3. Sutherland, F.W.H., Perry, T.E., Yu, Y., Sherwood, M.C., Rabkin, E., Masuda, Y., Garcia, G.A., McLellan, D.L., Engelmayr, Jr., G.C., Sacks, M.S., Schoen, F.J., and Mayer, Jr., J.E. From stem cells to viable autologous semilunar heart valve. Circulation **111,** 2783, 2005.
4. Stock, U.A., Nagashima, M., Khalil, P.N., Nollert, G.D., Herden, T., Sperling, J.S., Moran, A.M., Lien, J., Martin, D.P., Schoen, F.J., Vacanti, J.P., and Mayer, Jr., J.E. Tissue-engineered valved conduits in the pulmonary circulation. J Thorac Cardiovasc Surg **119,** 732, 2000.
5. Missirlis, Y.F., and Chong, M. Aortic valve mechanics–Part I: material properties of natural porcine aortic valves. J Bioeng **2,** 287, 1978.
6. Sauren, A.A.H.J., van Hout, M.C., van Steenhoven, A.A., Veldpaus, F.E., and Janssen, J.D. The mechanical properties of porcine aortic valve tissues. J Biomech **16,** 327, 1983.
7. Lee, J.M., Courtman, D.W., and Boughner, D.R. The glutaraldehyde-stabilized porcine aortic valve xenograft. I. Tensile viscoelastic properties of the fresh leaflet material. J Biomed Mater Res **18,** 61, 1984.
8. Nguyen, K.T., and West, J.L. Photopolymerizable hydrogels for tissue engineering applications. Biomaterials **23,** 4307, 2002.
9. Cruise, G.M., Scharp, D.S., and Hubbell, J.A. Characterization of permeability and network structure of interfacially photopolymerized poly(ethylene glycol) diacrylate hydrogels. Biomaterials **19,** 1287, 1998.
10. Mann, B.K., Gobin, A.S., Tsai, A.T., Schmedlen, R.H., and West, J.L. Smooth muscle cell growth in photopolymerized hydrogels with cell adhesive and proteolytically degradable domains: synthetic ECM analogs for tissue engineering. Biomaterials **22,** 3045, 2001.
11. Bahney, C.S., Lujan, T.J., Hsu, C.W., Bottlang, M., West, J.L., and Johnstone, B. Visible light photoinitiation of mesenchymal stem cell-laden bioresponsive hydrogels. Eur Cell Mater **22,** 43, 2011.
12. Nemir, S., Hayenga, H.N., and West, J.L. PEGDA hydrogels with patterned elasticity: novel tools for the study of cell response to substrate rigidity. Biotechnol Bioeng **105,** 636, 2010.
13. Tseng, H., Cuchiara, M.L., Durst, C.A., Cuchiara, M.P., Lin, C.J., West, J.L., and Grande-Allen, K.J. Fabrication and mechanical evaluation of anatomically-inspired quasi-laminate hydrogel structures with layer-specific formulations. Ann Biomed Eng **41,** 398, 2013.
14. Karpiak, J.V., Ner, Y., and Almutairi, A. Density gradient multilayer polymerization for creating complex tissue. Adv Mater **24,** 1466, 2012.
15. Hockaday, L.A., Kang, K.H., Colangelo, N.W., Cheung, P.Y.C., Duan, B., Malone, E., Wu, J., Girardi, L.N., Bonassar, L.J., Lipson, H., Chu, C.C., and Butcher, J.T. Rapid 3D printing of anatomically accurate and mechanically heterogeneous aortic valve hydrogel scaffolds. Biofabrication **4,** 035005, 2012.
16. Peyton, S.R., Raub, C.B., Keschrumrus, V.P., and Putnam, A.J. The use of poly(ethylene glycol) hydrogels to investigate the impact of ECM chemistry and mechanics on smooth muscle cells. Biomaterials **27,** 4881, 2006.
17. Del Gaudio, C., Bianco, A., and Grigioni, M. Electrospun bioresorbable trileaflet heart valve prosthesis for tissue engineering: *in vitro* functional assessment of a pulmonary cardiac valve design. Ann Ist Super Sanita **44,** 178, 2008.
18. Courtney, T., Sacks, M.S., Stankus, J.J., Guan, J., and Wagner, W.R. Design and analysis of tissue engineering scaffolds that mimic soft tissue mechanical anisotropy. Biomaterials **27,** 3631, 2006.
19. Pham, Q.P., Sharma, U., and Mikos, A.G. Electrospinning of polymeric nanofibers for tissue engineering applications: a review. Tissue Eng **12,** 1197, 2006.
20. Liu, W., Thomopoulos, S., and Xia, Y. Electrospun nanofibers for regenerative medicine. Adv Healthc Mater **1,** 10, 2012.
21. Han, N., Rao, S.S., Johnson, J., Parikh, K.S., Bradley, P.A., Lannutti, J.J., and Winter, J.O. Hydrogel-electrospun fiber mat composite coatings for neural prostheses. Front Neuroeng **4,** 2, 2011.
22. Han, N., Johnson, J., Lannutti, J.J., and Winter, J.O. Hydrogel-electrospun fiber composite materials for hydrophilic protein release. J Control Release **158,** 165, 2012.
23. Freeman, J.W., Woods, M.D., Cromer, D.A., Ekwueme, E.C., Andric, T., Atiemo, E.A., Bijoux, C.H., and Laurencin, C.T. Evaluation of a hydrogel-fiber composite for ACL tissue engineering. J Biomech **44,** 694, 2011.
24. Moutos, F.T., and Guilak, F. Functional properties of cell-seeded three-dimensionally woven poly(epsilon-caprolactone) scaffolds for cartilage tissue engineering. Tissue Eng Part A **16,** 1291, 2010.
25. Xu, W., Ma, J., and Jabbari, E. Material properties and osteogenic differentiation of marrow stromal cells on fiber-reinforced laminated hydrogel nanocomposites. Acta Biomater **6,** 1992, 2010.

26. Tomei, A.A., Boschetti, F., Gervaso, F., and Swartz, M.A. 3D collagen cultures under well-defined dynamic strain: a novel strain device with a porous elastomeric support. Biotechnol Bioeng **103,** 217, 2009.
27. Bosworth, L.A., Turner, L.-A., and Cartmell, S.H. State of the art composites comprising electrospun fibres coupled with hydrogels: a review. Nanomedicine **9,** 322, 2013.
28. Tseng, H., and Grande-Allen, K.J. Elastic fibers in the aortic valve spongiosa: a fresh perspective on its structure and role in overall tissue function. Acta Biomater **7,** 2101, 2011.
29. Chaudhuri, B.B., Kundu, P., and Sarkar, N. Detection and gradation of oriented texture. Pattern Recognit Lett **14,** 147, 1993.
30. Karlon, W.J., Covell, J.W., McCulloch, A.D., Hunter, J.J., and Omens, J.H. Automated measurement of myofiber disarray in transgenic mice with ventricular expression of ras. Anat Rec **252,** 612, 1998.
31. Sarkar, S., Isenberg, B.C., Hodis, E., Leach, J.B., Desai, T.A., and Wong, J.Y. Fabrication of a layered microstructured polycaprolactone construct for 3-D tissue engineering. J Biomater Sci Polym Ed **19,** 1347, 2008.
32. Hahn, M.S., McHale, M.K., Wang, E., Schmedlen, R.H., and West, J.L. Physiologic pulsatile flow bioreactor conditioning of poly(ethylene glycol)-based tissue engineered vascular grafts. Ann Biomed Eng **35,** 190, 2007.
33. Hoffmann, J.C., and West, J.L. Three-dimensional photolithographic micropatterning: a novel tool to probe the complexities of cell migration. Integr Biol (Camb) **5,** 817, 2013.
34. Taylor, P.M., Batten, P., Brand, N.J., Thomas, P.S., and Yacoub, M.H. The cardiac valve interstitial cell. Int. J Biochem Cell Biol **35,** 113, 2003.
35. Stephens, E.H., Carroll, J.L., and Grande-Allen, K.J. The use of collagenase III for the isolation of porcine aortic valvular interstitial cells: rationale and optimization. J Heart Valve Dis **16,** 175, 2007.
36. Liu Tsang, V., Chen, A.A., Cho, L.M., Jadin, K.D., Sah, R.L., DeLong, S., West, J.L., and Bhatia, S.N. Fabrication of 3D hepatic tissues by additive photopatterning of cellular hydrogels. FASEB J **21,** 790, 2007.
37. Durst, C.A., Cuchiara, M.P., Mansfield, E.G., West, J.L., and Grande-Allen, K.J. Flexural characterization of cell encapsulated PEGDA hydrogels with applications for tissue engineered heart valves. Acta Biomater **7,** 2467, 2011.
38. Rouxhet, L., Duhoux, F., Borecky, O., Legras, R., and Schneider, Y.-J. Adsorption of albumin, collagen, and fibronectin on the surface of poly(hydroxybutyrate-hydroxyvalerate) (PHB/HV) and of poly (epsilon-caprolactone) (PCL) films modified by an alkaline hydrolysis and of poly(ethylene terephtalate) (PET) track-etched membr. J Biomater Sci Polym Ed **9,** 1279, 1998.
39. Drevelle, O., Bergeron, E., Senta, H., Lauzon, M.-A., Roux, S., Grenier, G., and Faucheux, N. Effect of functionalized polycaprolactone on the behaviour of murine preosteoblasts. Biomaterials **31,** 6468, 2010.
40. Wang, Z., Teo, E.Y., Chong, M.S.K., Zhang, Q.-Y., Lim, J., Zhang, Z., Hong, M., Thian, E.-S., Chan, J.K.Y., and Teoh, S.-H. Biomimetic three-dimensional anisotropic geometries by uniaxial stretch of poly(ε-caprolactone) films for mesenchymal stem cell proliferation, alignment, and myogenic differentiation. Tissue Eng Part C Methods **19,** 2013.
41. Serrano, M.-C., Pagani, R., Vallet-Regí, M., Peña, J., Comas, J.-V., and Portolés, M.-T. Nitric oxide production by endothelial cells derived from blood progenitors cultured on NaOH-treated polycaprolactone films: a biofunctionality study. Acta Biomater **5,** 2045, 2009.
42. Tseng, H., Kim, E.J., Connell, P.S., Ayoub, S., Shah, J.V., and Grande-Allen, K.J. The tensile and viscoelastic properties of aortic valve leaflets treated with a hyaluronidase gradient. Cardiovasc Eng Technol **4,** 151, 2013.
43. Vesely, I., and Noseworthy, R. Micromechanics of the fibrosa and the ventricularis in aortic valve leaflets. J Biomech **25,** 101, 1992.
44. Vesely, I., and Lozon, A. Natural preload of aortic valve leaflet components during glutaraldehyde fixation: effects on tissue mechanics. J Biomech **26,** 121, 1993.
45. Quinlan, A.M.T., and Billiar, K.L. Investigating the role of substrate stiffness in the persistence of valvular interstitial cell activation. J Biomed Mater Res A **100,** 2474, 2012.
46. Throm Quinlan, A.M., Sierad, L.N., Capulli, A.K., Firstenberg, L.E., and Billiar, K.L. Combining dynamic stretch and tunable stiffness to probe cell mechanobiology *in vitro*. PLoS One **6,** e23272, 2011.
47. Walker, G.A., Masters, K.S., Shah, D.N., Anseth, K.S., and Leinwand, L.A. Valvular myofibroblast activation by transforming growth factor-β: implications for pathological extracellular matrix remodeling in heart valve disease. Circ Res **95,** 253, 2004.
48. Osman, L., Yacoub, M.H., Latif, N., Amrani, M., and Chester, A.H. Role of human valve interstitial cells in valve calcification and their response to atorvastatin. Circulation **114,** I547, 2006.
49. Rajamannan, N.M., Subramaniam, M., Rickard, D., Stock, S.R., Donovan, J., Springett, M., Orszulak, T.A., Fullerton, D.A., Tajik, A.J., Bonow, R.O., and Spelsberg, T.C. Human aortic valve calcification is associated with an osteoblast phenotype. Circulation **107,** 2181, 2003.
50. Sun, H., Mei, L., Song, C., Cui, X., and Wang, P. The *in vivo* degradation, absorption and excretion of PCL-based implant. Biomaterials **27,** 1735, 2006.
51. Chou, A.I., Akintoye, S.O., and Nicoll, S.B. Photo-cross-linked alginate hydrogels support enhanced matrix accumulation by nucleus pulposus cells *in vivo*. Osteoarthritis Cartilage **17,** 1377, 2009.
52. Nguyen, T.D., Liang, R., Woo, S.L.-Y., Burton, S.D., Wu, C., Almarza, A.J., Sacks, M.S., and Abramowitch, S. Effects of cell seeding and cyclic stretch on the fiber remodeling in an extracellular matrix-derived bioscaffold. Tissue Eng Part A **15,** 957, 2009.
53. Gould, R.A., Chin, K., Santisakultarm, T.P., Dropkin, A., Richards, J.M., Schaffer, C.B., and Butcher, J.T. Cyclic strain anisotropy regulates valvular interstitial cell phenotype and tissue remodeling in three-dimensional culture. Acta Biomater **8,** 1710, 2012.
54. Tedder, M.E., Simionescu, A., Chen, J., Liao, J., and Simionescu, D.T. Assembly and testing of stem cell-seeded layered collagen constructs for heart valve tissue engineering. Tissue Eng Part A **17,** 25, 2011.

Address correspondence to:
K. Jane Grande-Allen, PhD
Department of Bioengineering
Rice University
P.O. Box 1892–MS 142
Houston, TX 77251-1892

E-mail: grande@rice.edu

Received: June 30, 2013
Accepted: March 19, 2014
Online Publication Date: July 15, 2014